

A notion of depth for sparse functional data

Carlo Sguera* and Sara López-Pintado†

Abstract

Data depth is a well-known and useful nonparametric tool for analyzing functional data. It provides a novel way of ranking a sample of curves from the center outwards and defining robust statistics, such as the median or trimmed means. It has also been used as a building block for functional outlier detection methods and classification. Several notions of depth for functional data were introduced in the literature in the last few decades. These functional depths can only be directly applied to samples of curves measured on a fine and common grid. In practice, this is not always the case, and curves are often observed at sparse and subject dependent grids. In these scenarios the usual approach consists in estimating the trajectories on a common dense grid, and using the estimates in the depth analysis. This approach ignores the uncertainty associated with the curves estimation step. Our goal is to extend the notion of depth so that it takes into account this uncertainty. Using both functional estimates and their associated confidence intervals, we propose a new method that allows the curve estimation uncertainty to be incorporated into the depth analysis. We describe the new approach using the modified band depth although any other functional depth could be used. The performance of the proposed methodology is illustrated using simulated curves in different settings where we control the degree of sparsity. Also a real data set consisting of female medflies egg-laying trajectories is considered. The results show the benefits of using uncertainty when computing depth for sparse functional data.

Keywords: Sparse functional data; Data depth; Modified band depth; Functional principal component analysis.

*UC3M-Santander Big Data Institute, Universidad Carlos III de Madrid, Getafe, Spain. E-mail: carlo.sguera@uc3m.es.

†Department of Health Sciences, Northeastern University, Boston, USA. E-mail: s.lopez-pintado@northeastern.edu. Partial support from the National Institute of Mental Health (grant number: 1R21MH120534-01) is acknowledged.

1 Introduction and Motivation

Functional data analysis is an exciting developing area in statistics where the basic unit of observation is a function/curve. Many different statistical methods, such as principal components, analysis of variance, and linear regression, have been extended to functional data. In the last two decades there has been an intensive development of different notions of data depth which have been proven to be a powerful nonparametric tool for analyzing functional data. In general, a data depth is a function that measures the centrality (or outlyingness) of an observation within a population or sample. It provides a novel way of ranking observations from the center outwards and allows the definition of robust statistics such as medians, trimmed means and central regions for functional data. Moreover, data depth is often used as a building block for developing classification and outlier-detection techniques. Several notions of depth for functional data have been introduced in the literature (e.g., Fraiman and Muniz (2001), Cuevas et al. (2007), Cuesta-Albertos and Nieto-Reyes (2008), López-Pintado and Romo (2009), López-Pintado and Romo (2011) or Sguera et al. (2014)). Functional depths have been originally proposed for sample of curves that are measured on a common and dense grid. In practice, curves are often observed at subject-dependent and/or sparse grids. The main approach in the literature for dealing with this situation is based on estimating the individual trajectories on an artificially chosen common dense grid of points and using these estimated curves as observed data in a depth analysis (e.g., López-Pintado and Wei (2011)). Up to now, a functional depth analysis usually ignores the inherent uncertainty associated with the preliminary curve estimation step. In this paper we propose a general approach for calculating the depth of sparsely observed functions and we take uncertainty into account by analyzing with a depth function both functional estimates and their associated confidence intervals.

We present the new approach using: (1) the modified band depth (MBD , López-Pintado and Romo (2009)) as functional depth; (2) the iterated expectation and variance method (IEV , Goldsmith et al. (2013)) to obtain estimates and confidence intervals. Note that the proposed methodology can be generalized to any functional depth and to any curve estimation method that provides confidence intervals. The paper is arranged as follows: in Section 2 we give a general overview of the notion of functional depth focusing on MBD . In Section 3 we propose the novel approach to compute the depth of sparse functional data taking into account the uncertainty in the estimation and define a new version of MBD that we call “modified band depth under uncertainty” (MBD_U). Section 4 shows the performance of MBD_U in a simulation study where curves with different degrees of sparsity are generated. In Section 5 we use MBD_U in a real data example consisting of female medflies egg-laying trajectories (Carey et al. (1998)).

2 The modified band depth

Given a probability distribution, a statistical depth assigns to each point a real non-negative bounded value that measures the centrality of the point with respect to its distribution. Several depth definitions for multivariate data have been proposed and analyzed by Mahalanobis (1936), Tukey (1975), Oja (1983), Liu et al. (1990), Liu and Singh (1993), Chaudhuri (1996), Koshevoy et al. (1997), Liu et al. (1999), Rousseeuw and Hubert (1999), Vardi and Zhang (2000) and Zuo (2003) among others. Liu et al. (1990) and Zuo and Serfling (2000) introduced and studied key properties a depth should satisfy. However, most of these depths are computationally intractable and not well defined in high-dimensions and functional spaces.

In the last two decades several notions of depth have been proposed for functional data

(see, e.g., Fraiman and Muniz (2001); López-Pintado and Romo (2007), Cuesta-Albertos and Nieto-Reyes (2008), López-Pintado and Romo (2009), López-Pintado and Romo (2011); López-Pintado and Jörnsten (2007), Cuevas et al. (2007); Gervini (2012), Sguera et al. (2014), Chakraborty and Chaudhuri (2014), Narisetty and Nair (2016), among others). Functional depths provide a novel way of ranking functions from the center outwards and robust location estimators such as median or trimmed means can be defined using depth functions. Moreover, those curves from the sample with low depth can be considered as potential outliers and depth-based outlier detection rules for functional data have been recently introduced in the literature (see, e.g., Hubert et al. (2015), Arribas-Gil and Romo (2014) and Sun and Genton (2011), Dai and Genton (2017), Sguera et al. (2016), Azcorra et al. (2018), among others). Also, robust nonparametric tests for functional data based on functional depths have been proposed in the literature (see, e.g., López-Pintado and Romo (2009), Sun and Genton (2012), López-Pintado and Wrobel (2017), Flores et al. (2018)). The notion of depth can also be used for developing nonparametric classification methods (see e.g., Jörnsten (2004), Li et al. (2012), Sguera et al. (2014) and Cuesta-Albertos et al. (2017)).

In this paper we focus on the modified band depth for functional data introduced in López-Pintado and Romo (2009), which is based on the graphic representation of the curves. It satisfies desirable theoretical properties and is computationally fast. It provides a natural and novel way of ordering curves from the center outwards, and can be used to generalize classical order statistics to functional data.

Let $(\mathcal{C}(I), \mathcal{P})$ be the space of continuous real valued functions on the compact interval $I \in \mathbb{R}$ with the supremum norm $\|\cdot\|_\infty$ and the probability measure \mathcal{P} . The modified band depth of a function y in $(\mathcal{C}(I), \mathcal{P})$ is defined as $MBD(y, \mathcal{P}) = E_{Y_1, Y_2}[\lambda(A(y; Y_1, Y_2))]$, where $\lambda = \frac{\lambda_L}{\lambda_L(I)}$, λ_L is Lebesgue measure in \mathbb{R} and

$$A(y; Y_1, Y_2) = \left\{ s \in I : \min_{j=1,2} Y_j(s) \leq y(s) \leq \max_{j=1,2} Y_j(s) \right\}. \quad (1)$$

Basically, $MBD(y, \mathcal{P})$ measures how long the curve y is expected to be inside a stochastic band determined by two random functions Y_1 and Y_2 from $(\mathcal{C}, \mathcal{P})$. By Fubini's theorem one can express MBD as

$$MBD(y; \mathcal{P}) = \int_{\mathcal{I}} SD(y(s); \mathcal{P}_{Y(s)}) ds, \quad (2)$$

where

$$SD(y(s); \mathcal{P}_{Y(s)}) = P(\min(Y_1(s), Y_2(s)) \leq y(s) \leq \max(Y_1(s), Y_2(s)))$$

is the standard univariate simplicial depth of y at location s . MBD can be computed in a very fast and efficient way using the algorithm in Sun and Genton (2012).

Let $Y_i(s)$, with $1 \leq i \leq n$, be a sample of n functions from $(\mathcal{C}(I), \mathcal{P})$, and denote this sample as $\mathbf{Y} = \{Y_i(s)\}_{i=1}^n$. The sample modified band depth of a given curve Y_i with respect to the whole functional data set \mathbf{Y} is given by

$$MBD(Y_i; \mathbf{Y}) = \binom{n}{2}^{-1} \sum_{1 \leq i_1 \leq i_2 \leq n} \lambda(A(Y_i; Y_{i_1}, Y_{i_2})). \quad (3)$$

Intuitively, the sample modified band depth ($MBD(Y_i; \mathbf{Y})$) measures in average for how long the function Y_i is contained in the band determined by any two functions Y_{i_1}, Y_{i_2} from the sample. It can be seen as a measure of centrality/similarity between Y_i and the sample curves. The modified band depth satisfies natural and desirable depth properties such as: non-degeneracy, invariance, maximality at center, decreasing with respect to the deepest point, semi-continuity, and consistency. See Table 1 in Gijbels and Nagy (2017) for details

about these properties and comparisons with other depth notions. Mosler and Polyakova (2012) and Nieto-Reyes and Battey (2016) provide more discussion on functional data depth properties.

To apply the notion of depth to a sample of functions, the curves have to be evaluated at the same regular grid. In practice, this is rarely the case, since many times the functions are observed at different sparse points, and therefore a preliminary step to estimate the sample functions in a common fine grid is needed. In the next section we propose an approach to calculate the depth of sparse functions taking into account the uncertainty in the estimation of the curves, and we implement it using *MBD*. Note that our approach could be applied to any notion of functional depth.

3 A new modified band depth under uncertainty

Although no official definition exists of “dense” or “sparse” functional data, generally, if the number of observed points per curve is larger than some order of the sample size, n , then the functional data are referred to as “dense” (see Zhang and Wang (2016) for a detailed discussion on this topic). Nevertheless, even if the data is dense, some preliminary step is usually needed to have the sample defined on the same common grid of points when the curves are observed at subject specific grid or to denoise the observed sample. As observed by Yao et al. (2005), individual smoothing of the curves when data are sparse in general does not work well, and therefore the curves need to be estimated borrowing information from other curves. They proposed a method to reconstruct functional observations from sparse data which relies on functional principal components (FPC) analysis. Goldsmith et al. (2013) modified the method proposed by Yao et al. (2005) defining a bootstrap-based version which accounts for uncertainty in the FPC decomposition and

is known as iterated expectation and variance method. IEV is the method we use to reconstruct functional data and obtain confidence intervals of such estimates. All the details about IEV are reported in the appendix.

To show the differences between dealing with densely or sparsely observed functional data, see Figures 1 and 2.

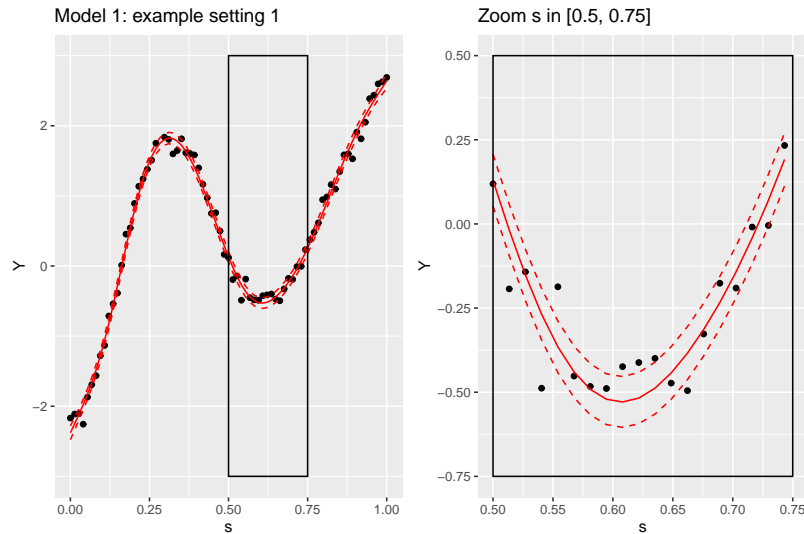


Figure 1: Example of densely observed functional data evaluated at black points together with its *IEV* estimate (solid line) and 95% confidence interval (dashed lines) (left). Same example zoomed in and showing only a proportion of the domain (right).

To obtain Figures 1 and 2 we have considered a simulation model (Model 1) and two simulation settings (settings 1 and 4, respectively) that we present in detail in Section 4. In Figure 1 we represent a densely observed curve together with its associated IEV estimate and 95% confidence intervals. In Figure 2 we represent a sparsely observed curve together with its associated IEV estimate and 95% confidence intervals. In the dense case there is little estimation uncertainty and the confidence interval is so narrow that it is hard to

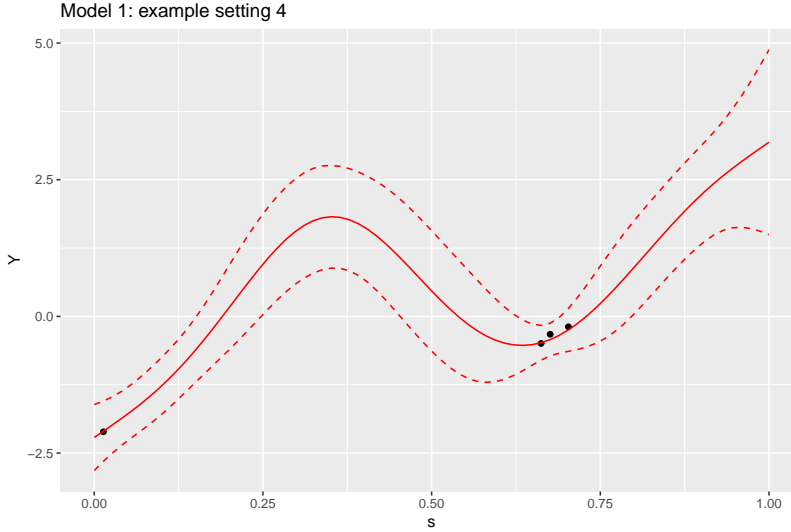


Figure 2: Example of sparsely observed functional data evaluated at black points together with its *IEV* estimate (solid line) and 95% confidence interval (dashed lines).

appreciate. For this reason we also zoom in on a portion of the domain. In the sparse case there is a lot of estimation uncertainty and the confidence interval is very wide.

Figures 1 and 2 illustrate the differences between dense and sparse functional data. Our next goal is to present a new depth that does not depend only on the estimated curves but also on their associated confidence intervals.

Let $\tilde{\mathbf{Y}}$ be a functional data set consisting of functions that are observed with measurement error and on different subject specific finite grids which could be irregularly spaced. We use *IEV* to obtain curves estimates and confidence intervals for $\tilde{\mathbf{Y}}$. Let $\hat{\mathbf{Y}}$ be the functional data set containing the curves estimates provided by *IEV* when applied to $\tilde{\mathbf{Y}}$. Similarly, let $\hat{\mathbf{Y}}_{ub}$ and $\hat{\mathbf{Y}}_{lb}$ be the functional data sets composed by the confidence intervals upper and lower bounds, respectively. Note that estimates and confidence intervals are evaluated on a common and dense grid denoted as \mathbf{s}_g .

When performing a data depth analysis on $\tilde{\mathbf{Y}}$, a standard approach consists on simply applying any depth function, for example MBD , to $\hat{\mathbf{Y}}$. We propose to take into account that $\hat{\mathbf{Y}}$ is the result of a preliminary estimation step and incorporate in the depth analysis its related uncertainty. In particular, we propose to include the information contained in $\hat{\mathbf{Y}}_{ub}$ and $\hat{\mathbf{Y}}_{lb}$ in the following way: first, create the auxiliary enlarged functional data set of size $3n$, $\hat{\mathbf{Y}}_U$, defined as the union of $\hat{\mathbf{Y}}_{ub}$, $\hat{\mathbf{Y}}$ and $\hat{\mathbf{Y}}_{lb}$; second, compute MBD for $\hat{\mathbf{Y}}_U$; third, assign the following depth value to each $\hat{Y}_i(\mathbf{s}_g) = \hat{Y}_i$:

$$MBD_U(\hat{Y}_i; \hat{\mathbf{Y}}) = \frac{MBD(\hat{Y}_{ub,i}; \hat{\mathbf{Y}}_U) + MBD(\hat{Y}_i; \hat{\mathbf{Y}}_U) + MBD(\hat{Y}_{lb,i}; \hat{\mathbf{Y}}_U)}{3}, \quad (4)$$

where $\hat{Y}_{lb,i} = \hat{Y}_{lb,i}(\mathbf{s}_g)$ and $\hat{Y}_{ub,i} = \hat{Y}_{ub,i}(\mathbf{s}_g)$. Note that $MBD_U(\hat{Y}_i; \hat{\mathbf{Y}})$ is defined as the average depth with respect to $\hat{\mathbf{Y}}_U$ of three functions: the estimated curve, the confidence interval upper bound and the confidence interval lower bound. By using these elements, MBD_U is taking into account the estimation uncertainty, and therefore our proposal represents an alternative to the standard approach, $MBD(\hat{Y}_i; \hat{\mathbf{Y}})$, which only depends on the curves estimates.

So far we are omitting that MBD_U depends on a tuning parameter $\alpha \in (0, 1)$ which controls the width of the $100(1 - \alpha)\%$ confidence intervals. Although, we have shown that for a given α , the confidence interval is wider when the curve is more sparsely observed. Moreover, in a preliminary study we have observed that for a given functional sample:

- low values of α generate very wide intervals and versions of MBD_U that give too much weight to estimation uncertainty.
- high values of α generate too narrow intervals and versions of MBD_U that resemble

excessively to MBD .

Let $MBD_{U,\alpha}(\hat{Y}_i; \hat{Y})$ be the version of (4) that we obtain using a given α . Seeking for a version of MBD_U that systematically employs intermediate values of α , we have defined the following procedure to set α :

1. Given \tilde{Y} and estimated \hat{Y} using *IEV*, compute $MBD_{U,\alpha}(\hat{Y}_i; \hat{Y})$ for $\alpha \in \{0.05, 0.06, \dots, 0.98, 0.99\}$ and each observation ($1 \leq i \leq n$). Moreover, compute $MBD(\hat{Y}_i; \hat{Y})$ for each observation. Let $MBD_{U,\alpha}(\hat{Y})$ be the sample depth values obtained using our proposal and $MBD(\hat{Y})$ be the sample depth values obtained using MBD applied only to the curves estimates.
2. For each $\alpha \in \{0.05, 0.06, \dots, 0.98, 0.99\}$, compute the Spearman rank correlation coefficient ρ_S between $MBD(\hat{Y})$ and $MBD_{U,\alpha}(\hat{Y})$, i.e., $\rho_S(\hat{Y}; \alpha) = \rho_S(MBD(\hat{Y}), MBD_{U,\alpha}(\hat{Y}))$. In what follows we omit the subscript S to refer to the Spearman rank correlation coefficient, hence $\rho_S = \rho$.
3. Let α^* be the largest α such that

$$\rho(\hat{Y}; \alpha) \leq 0.95. \quad (5)$$

If α^* exists, use α^* and compute $MBD_{U,\alpha^*}(\hat{Y})$. If α^* does not exist, do not compute $MBD_{U,\alpha}(\hat{Y})$.

Note that the larger α the narrower the confidence intervals and the closer is MBD_U to MBD . This procedure explores different versions of MBD_U , from versions that use wide confidence intervals (low values of α) and give more importance to estimation uncertainty, to versions that use narrow confidence intervals (high values of α). Note that α^* is chosen

in a data-driven way, looking at the relationship between $MBD(\hat{\mathbf{Y}})$ and $MBD_{U,\alpha}(\hat{\mathbf{Y}})$. The relationship is analyzed using Spearman rank correlation coefficients because the ranking is certainly one of the most valuable outputs on any depth analysis. This analysis is done searching for a value of α such that $MBD(\hat{\mathbf{Y}})$ and $MBD_{U,\alpha}(\hat{\mathbf{Y}})$ differ between them, but not excessively (for this reason we set the threshold for ρ to 0.95). If α^* exists, we argue that $MBD_{U,\alpha^*}(\hat{\mathbf{Y}})$ might be preferable to $MBD(\hat{\mathbf{Y}})$ since it is taking estimation uncertainty into account. If α^* does not exist, there is no need to use $MBD_{U,\alpha}(\hat{\mathbf{Y}})$ instead of $MBD(\hat{\mathbf{Y}})$ since they never differ excessively. Note that the computational cost to set α^* is negligible with respect to the computational cost of obtaining the bootstrap-based *IEV* estimates, which is a step required by both the standard approach, $MBD(\hat{\mathbf{Y}})$, and $MBD_{U,\alpha}(\hat{\mathbf{Y}})$.

In the next section we use an extensive simulation study to compare the behavior of MBD and MBD_U .

4 Simulation study

In this section we present the results of a simulation study designed to evaluate the performance of MBD_U in different settings. We consider the models described in Zhang and Wang (2016) to generate functional data. Four settings with different degrees of sparsity are considered for generating the number of observed evaluation points, J_i , $i = 1, \dots, n$:

- Setting 1: J_i are i.i.d. from a discrete uniform distribution on the set $\{\lfloor n/8 \rfloor, \lfloor (n+1)/8 \rfloor, \dots, \lfloor 3n/8 \rfloor\}$ where $\lfloor x \rfloor$ indicates the integer part of x .
- Setting 2: $J_i = n/4$ or i.i.d from a discrete uniform distribution on the set $\{2, 3, 4, 5\}$ with equal probability.

- Setting 3: $J_i = n/4$ or i.i.d from a discrete uniform distribution on the set $\{2, 3, 4, 5\}$ with probability equal to $n^{-1/4}$ and $1 - n^{-1/4}$, respectively.
- Setting 4: J_i are i.i.d. from a discrete uniform distribution on the set $\{2, 3, 4, 5\}$.

Setting 1 provides dense data while setting 4 provides sparse data. Settings 2 and 3 provide dense and sparse data with the difference that under setting 2 approximately half observations are dense and half are sparse while under setting 3 the majority of observations are sparse. Nevertheless, in all settings curves are observed on grids that usually differ from one curve to another, and therefore it is always necessary to estimate them on a common grid. We use *IEV* to obtain the estimates, and the number of bootstrap iterations that we use is 100.

Following the ideas of Zhang and Wang (2016), we use as model 1 a model with true mean and covariance functions defined as follows:

$$\mu(s) = \frac{3}{2} \sin\left(3\pi\left(s + \frac{1}{2}\right)\right) + 2s^3, \quad \Sigma(s, s') = \sum_{k=1}^4 \lambda_k \phi_k(s) \phi_k(s'), \quad s, s' \in [0, 1], \quad (6)$$

where $\lambda_k = 1/(k+1)^2, k = 1, \dots, 4$ and

$$\begin{aligned} \phi_1(s) &= \sqrt{2} \cos(2\pi s), \quad \phi_2(s) = \sqrt{2} \sin(2\pi s), \\ \phi_3(s) &= \sqrt{2} \cos(4\pi s), \quad \phi_4(s) = \sqrt{2} \sin(4\pi s). \end{aligned}$$

Then, functional data are generated using

$$\tilde{Y}_i(s) = Y_i(s) + \epsilon_i(s) = \mu(s) + \sum_{k=1}^4 \xi_{ik} \phi_k(s) + \epsilon_i(s), \quad 1 \leq i \leq n, \quad (7)$$

where ξ_{ik} are i.i.d from $N(0, \lambda_k)$ and $\epsilon_i(s)$ are i.i.d from $N(0, 0.01)$, and independent between them.

We use model 1 in the following way: first, we generate $n = 200$ functional data evaluated at $\lfloor 3n/8 \rfloor = 75$ equidistant points in $[0, 1]$. Then, we apply settings from 1 to 4 to obtain dense and sparse scenarios. Once a setting is applied, we use *IEV* to reconstruct the curves and build the confidence intervals. In Figure 3 we report an example of a functional data set before applying any setting (left), its *IEV* estimates after applying setting 1 (center) and its *IEV* estimates after applying setting 4 (right).

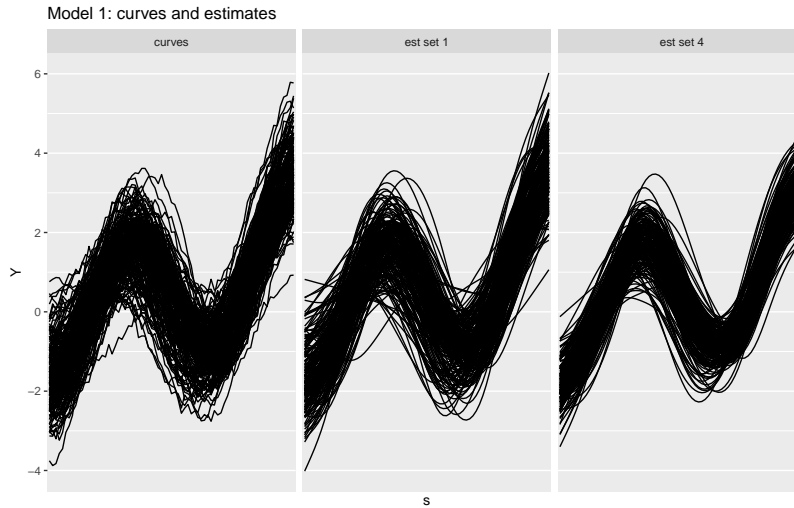


Figure 3: Functional data set generated by model 1 (left). *IEV* estimates of the curves generated from model 1 after applying setting 1 (center). *IEV* estimates of the curves generated from model 1 after applying setting 4 (right).

Observing Figure 3 it is possible to appreciate some minor differences between the

curves estimates under setting 1 (Figure 3, center) and under setting 4 (Figure 3, right). Note that we appreciate more difference between these two very different sparse setting if we consider the IEV confidence intervals (Figures 1 and 2) instead of just the estimates (Figure 3).

To illustrate the differences between MBD and MBD_U , we have computed both depth measures for the estimated curves in Figure 3 under setting 1 (center panel) and setting 4 (right panel). For this example we use $\alpha = 0.05$ to obtain standard 95% confidence intervals. Figure 4 shows the scatter plots of “ MBD versus MBD_U ” under setting 1 and 4 in the left and right panel, respectively.

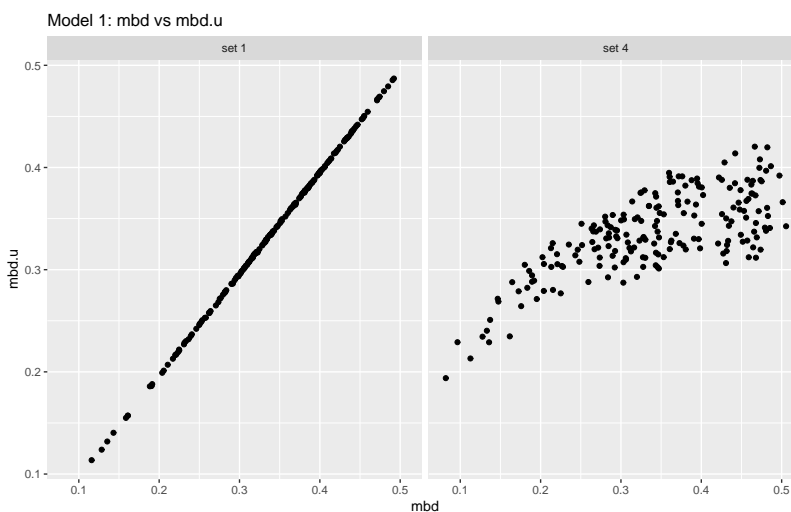


Figure 4: Scatter plots of $(MBD(\hat{Y}), MBD_{U,0.05}(\hat{Y}))$ obtained after implementing setting 1 (left) and setting 4 (right) to a functional data set generated from model 1.

From Figure 4 it can be seen that when data are densely observed in practice there is no difference between MBD and MBD_U since the degree of uncertainty is low (Figure 4, left). However, when data are sparsely observed the degree of uncertainty is higher and we

observe differences between MBD and MBD_U (Figure 4, right).

To further explore these differences and analyze which depth approach performs better, we use a simulation study in which we simulate 100 data sets using model 1 and apply each one of the settings. For each data set generated by model 1, say $\tilde{\mathbf{Y}}$, and before implementing settings 1-4, we compute the “true” depth $MBD(\mathbf{Y})$, i.e., the depth values obtained using MBD and \mathbf{Y} , the functional data set without measurement errors $\epsilon_i(s)$. Then, after generating $\tilde{\mathbf{Y}}$ under each setting and using IEV , we compute $MBD(\hat{\mathbf{Y}})$ and $MBD_{U,\alpha^*}(\hat{\mathbf{Y}})$, and their respective Spearman rank correlation coefficients with respect to the benchmark $MBD(\mathbf{Y})$, that is, $\rho_0 = \rho(MBD(\mathbf{Y}), MBD(\hat{\mathbf{Y}}))$ and $\rho_U = \rho(MBD(\mathbf{Y}), MBD_{U,\alpha^*}(\hat{\mathbf{Y}}))$. Recall that α^* is set using the data-driven procedure described in Section 3. Therefore, for each pair model-setting, we observe 100 values of ρ_0 and ρ_U , and also α^* . In Figure 5 we report all the pairs (ρ_0, ρ_U) . The different types of points indicate the different settings.

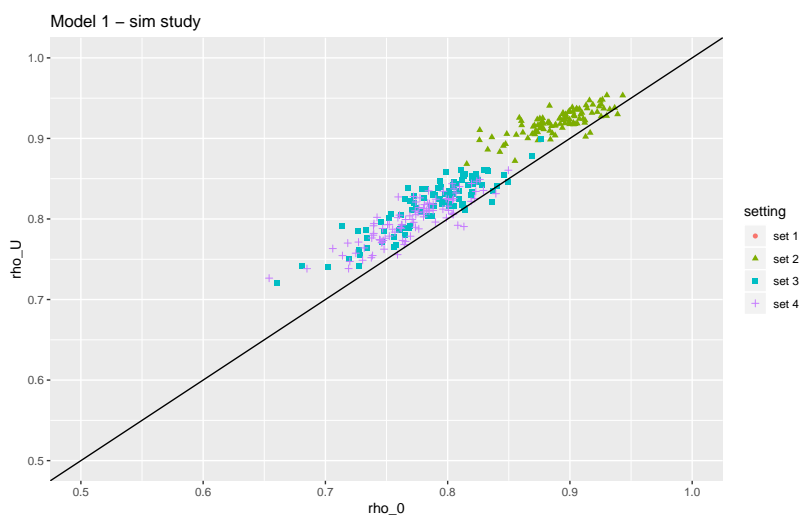


Figure 5: Model 1: scatter plot of (ρ_0, ρ_U) under settings 1-4.

In Figure 5 there are no points associated to setting 1, and this is due to the fact that according to the procedure to set α presented in Section 3 there is no α such that (5) holds,

and therefore MBD and MBD_U provide very similar rankings in this dense setting and there is no need to use MBD_U . For the rest of the settings almost all the points are above the diagonal, indicating a consistent better performance of MBD_U with respect to MBD .

To provide more information, in Table 1 we report the median values of ρ_0 , ρ_U , the quantity $\Delta_\rho = \frac{\rho_U - \rho_0}{\rho_0} \times 100\%$ and α^* .

	median values			
	ρ_0	ρ_U	Δ_ρ	α^*
setting 1	1.00	-	-	-
setting 2	0.89	0.92	3.34%	0.23
setting 3	0.79	0.82	3.83%	0.30
setting 4	0.77	0.80	3.61%	0.29

Table 1: Model 1: median values of ρ_0 , ρ_U , Δ_ρ and α^* under settings 1-4.

Based on Figure 5 and Table 1 we first notice something expected: both $MBD(\hat{\mathbf{Y}})$ and $MBD_{U,\alpha^*}(\hat{\mathbf{Y}})$ have a stronger relationship with the benchmark $MBD(\mathbf{Y})$ under setting 2, for which the median values of ρ_0 and ρ_U are 0.89 and 0.92, respectively. Under setting 3 the median values drop to 0.79 for ρ_0 and 0.82 for ρ_U , while under setting 4 they slightly decrease to 0.77 and 0.80, respectively. Moreover, these values and Figure 5 show that the overall performances of $MBD_{U,\alpha^*}(\hat{\mathbf{Y}})$ are better than the ones of $MBD(\hat{\mathbf{Y}})$, no matter the setting, which means that in general there is a stronger relationship between the benchmark $MBD(\mathbf{Y})$ and $MBD_{U,\alpha^*}(\hat{\mathbf{Y}})$ than with $MBD(\hat{\mathbf{Y}})$. Indeed, if for each data set we look at Δ_ρ , its median values are 3.34% (setting 2), 3.83% (setting 3) and 3.61% (setting 4). With respect to α^* , recall that under setting 1 α^* never exists, which means that $\rho(MBD(\hat{\mathbf{Y}}), MBD_{U,\alpha}(\hat{\mathbf{Y}}))$ is always greater than 0.95, while its median values are 0.23, 0.30 and 0.29 under settings 2, 3 and 4, respectively. To interpret this pattern, recall that, for a given α , IEV confidence intervals are naturally wider in sparse settings (see Figures 1 and 2). Therefore, the fact that the median value of α^* is lower in setting 2 than

in setting 3 or 4 means that our data-driven procedure is more conservative under sparse scenarios, and it selects lower confidence levels.

Besides model 1, we consider three additional models:

- Model 2 is obtained modifying the distribution of ξ_{ik} in (7): the scores ξ_{ik} are drawn with equal probability from either $N(-\sqrt{\frac{\lambda_k}{2}}, \lambda_k/2)$ or $N(\sqrt{\frac{\lambda_k}{2}}, \lambda_k/2)$. Model 2 is based on a model considered by Goldsmith et al. (2013).
- Model 3 is obtained modifying the set of λ_k in (7): $\lambda_k = 1/(k + 1), k = 1, \dots, 4$. Model 3 generates functional data using a truncated Karhunen-Loève expansion with more balanced components.
- Model 4 is obtained modifying the distribution of $\epsilon_i(s)$ in (7): $\epsilon_i(s)$ are i.i.d from $N(0, 0.02)$. Model 4 generates functional data that are observed with more noise than under model 1.

The results for models 2, 3 and 4 are reported in this section in Table 2 and in the appendix in Figures 8, 9 and 10.

Here we report the main findings on these additional models:

- Under setting 1 and models 2, 3 and 4, the procedure to set α for MBD_U always concludes that $MBD(\hat{\mathbf{Y}})$ and $MBD_{U,\alpha}(\hat{\mathbf{Y}})$ do not significantly differ for any considered α . Therefore, for all the considered models, when functional data are densely observed there is no need to use MBD_U instead of MBD^1 . Recall that such a decision is taken automatically and in a data-driven way using the proposed procedure to set α^* .

¹As a consequence, in the figures in the appendix there are no points for the scenarios “model 2-setting 1”, “model 3-setting 1” and “model 4-setting 1”.

		median values			
		ρ_0	ρ_U	Δ_ρ	α^*
model 2	setting 1	1.00	-	-	-
	setting 2	0.88	0.91	4.19%	0.23
	setting 3	0.76	0.80	4.39%	0.28
	setting 4	0.75	0.78	3.77%	0.29
model 3	setting 1	1.00	-	-	-
	setting 2	0.87	0.92	5.41%	0.27
	setting 3	0.76	0.80	6.06%	0.33
	setting 4	0.73	0.77	5.74%	0.36
model 4	setting 1	0.99	-	-	-
	setting 2	0.87	0.91	4.00%	0.24
	setting 3	0.76	0.80	4.22%	0.30
	setting 4	0.74	0.77	3.84%	0.31

Table 2: Model 2, 3 and 4: median values of ρ_0 , ρ_U , Δ_ρ and α^* under settings 1-4.

- For models 2, 3 and 4, both $MBD(\hat{\mathbf{Y}})$ and $MBD_{U,\alpha^*}(\hat{\mathbf{Y}})$ have a stronger relationship with the benchmark $MBD(\mathbf{Y})$ under setting 2 than under settings 3 or 4. Similar results were observed for model 1.
- As for model 1, the overall performances of $MBD_{U,\alpha^*}(\hat{\mathbf{Y}})$ are always better than the ones of $MBD(\hat{\mathbf{Y}})$ for all the new models and under settings 2, 3 and 4. If we consider again Δ_ρ , it ranges from 3.77% (“model 2-setting 4”) to 6.06% (“model 3-setting 3”).
- Finally, the pattern of higher α^* for more sparsely observed functional data is also observed under models 2, 3 and 4.

The simulation study presented in this section provides empirical evidence in favor of using MBD_U instead of the standard approach, specially with sparsely observed functional data. In the next section we consider a real functional data set to gather additional

information about MBD_U .

5 Real data application: medfly data set

Comparing MBD and MBD_U using a real sparse functional data set is a hard task since a benchmark distribution of depth values is missing. Therefore, our strategy consists on considering a real functional data set that has been observed sufficiently densely and might be affected by measurement error, say $\tilde{\mathbf{Y}}$, and induce sparsity on $\tilde{\mathbf{Y}}$. We use $MBD(\tilde{\mathbf{Y}})$ as the benchmark true depth to evaluate $MBD(\hat{\mathbf{Y}})$ and $MBD_{U;\alpha^*}(\hat{\mathbf{Y}})$, which are computed after inducing sparsity and applying IEV to estimate the curves and obtain the confidence intervals.

As $\tilde{\mathbf{Y}}$ we consider the medfly data set used in Carey et al. (1998). The data set consists on individual egg-laying counts during the first 25 days of lives for 789 female medflies (Mediterranean fruit flies, *Ceratitis capitata*) at the mass rearing facility in Metapa, Mexico. The medflies egg-laying trajectories are observed at a fix grid of days, $\mathbf{s}_g = \{1, \dots, 25\}$. In Figure 6 we represent the medfly data set (only a 10% random subsample is represented for graphical reasons).

We induce sparsity on the medfly data set using three different settings. In this case we focus on highly sparse settings:

- Each curve is observed at $J_i = 5$ random points from \mathbf{s}_g .
- Each curve is observed at J_i random points from \mathbf{s}_g , and J_i are i.i.d. from a discrete uniform distribution on the set $\{2, 3, 4, 5\}$.
- Each curve is observed at $J_i = 2$ random points from \mathbf{s}_g .

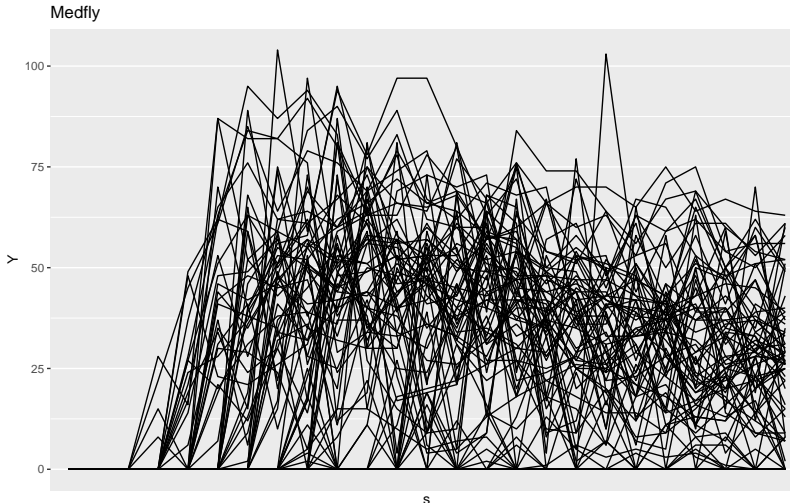


Figure 6: Medfly data set (10% of the observations).

As in the simulation study, for each setting we simulate 100 sparse data sets. The main difference with respect to the simulation study of Section 4 is that we have a unique sample to which we induce sparsity. Moreover, we observe $\tilde{\mathbf{Y}}$, i.e., a functional data set that has been possibly measured with error. Therefore $\tilde{\mathbf{Y}}$ is our benchmark data set. For each simulated sparse data set, after using IEV^2 , we compute $MBD(\hat{\mathbf{Y}})$ and $MBD_{U;\alpha^*}(\hat{\mathbf{Y}})$, and their correlations with the new benchmark $MBD(\tilde{\mathbf{Y}})$, i.e., $\rho_0 = \rho(MBD(\tilde{\mathbf{Y}}), MBD(\hat{\mathbf{Y}}))$ and $\rho_U = \rho(MBD(\tilde{\mathbf{Y}}), MBD_{U;\alpha^*}(\hat{\mathbf{Y}}))$. In Figure 7 we report all the pairs (ρ_0, ρ_U) , whereas in Table 3 we report the median values of $\rho_0, \rho_U, \Delta_\rho$ and α^* .

Based on the results shown in Figure 7 and Table 3 we can conclude that the settings with more sparsity show a lower correlation between both $MBD(\hat{\mathbf{Y}})$ and $MBD_{U;\alpha^*}(\hat{\mathbf{Y}})$, and the benchmark. Under the least sparse setting ($J_i = 5$), the performances of MBD and MBD_U are comparable, but in the remaining two settings we observe consistent improve-

²We constrain its estimates and confidence intervals to take non-negative values. We use this constrain to be coherent with the nature of the real problem and avoid negative egg-laying counts.

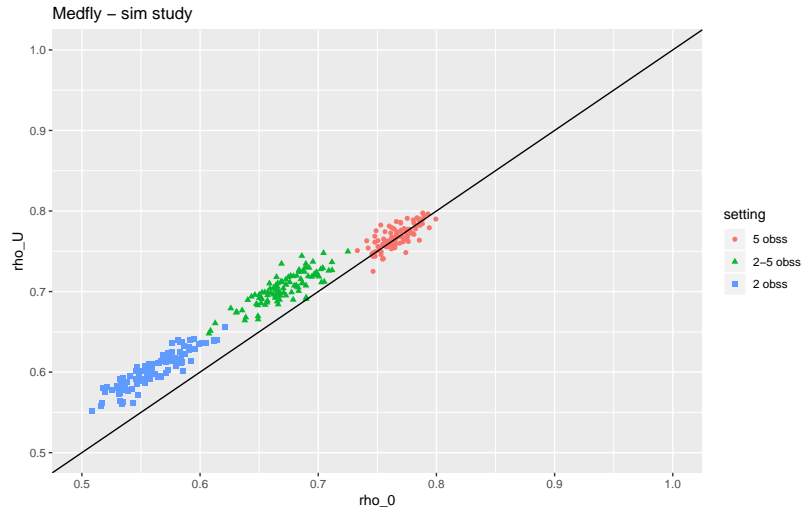


Figure 7: Medfly data set: scatter plot of (ρ, ρ_U) under different settings.

	median values			
	ρ_0	ρ_U	Δ_ρ	α^*
$J_i = 5$	0.77	0.77	0.07%	0.14
$J_i \in \{2, 3, 4, 5\}$	0.67	0.70	5.26%	0.35
$J_i = 2$	0.56	0.60	7.53%	0.42

Table 3: Medfly data set: median values of ρ_0 , ρ_U , Δ_ρ and α^* under different settings.

ments by using MBD_U . Note that in Figure 7 the points in the two very sparse scenarios are always above the diagonal line indicating a higher correlation between MBD_U and the benchmark than MBD and the benchmark. With respect to α^* , we observe a pattern that we have already highlighted in our simulation study: the proposed procedure selects lower confidence levels in relatively more sparse scenarios in a data-driven way.

Therefore, in very sparse settings our proposal, $MBD_{U;\alpha^*}(\hat{\mathbf{Y}})$, has consistently stronger association to the “true depth” $MBD(\tilde{\mathbf{Y}})$. This result is coherent with the ones found using simulated data, and support the need of taking into account uncertainty when applying depth to sparse functional data.

6 Conclusions

In this paper we have introduced a new approach for calculating depth values when functional data sets are sparsely observed. The standard approach consists of using any method for estimating the curves in a fine common grid, possibly borrowing information from the other curves in the sample, and applying a depth function to the estimated curves. We propose to take into account that the curves are estimated with uncertainty and incorporate this key aspect in the calculation of depth values. In particular, we use the *IEV* method to estimate the curves and their confidence intervals. Moreover, we propose MBD_U , a new functional depth based on MBD that takes into account both the curve estimates and confidence intervals. Therefore, MBD_U incorporates the uncertainty behind the estimation step required for sparse functional data. Finally, with both simulated and real data sets, we have shown the benefits of using MBD_U instead of MBD when computing the depth of sparse functional data. In particular, we have shown that MBD_U provides a ranking that is closer to the true underlying ranking.

A The iterated expectation and variance method

IEV assumes that: (1) the underlying curves $Y_i(s)$, $1 \leq i \leq n$, are defined in compact interval, $s \in I = [a, b] \subset \mathbb{R}$ and (2) are realizations of a random function with mean $\mu(s) = E[Y_i(s)]$ and covariance operator defined as $\Sigma^{\mathbf{Y}}(s, s') = Cov(Y_i(s), Y_i(s'))$. Based on the spectral decomposition of $\Sigma^{\mathbf{Y}}(s, s')$, a Karhunen-Loève expansion for $Y_i(s)$ can be defined as $Y_i(s) = \mu(s) + \sum_{k=1}^{\infty} \xi_{ik} \phi_k(s)$, where $\phi(s) = \{\phi_k(s) : k \in \mathbb{Z}^+\}$ are orthonormal eigenfunctions, $\lambda_1 \geq \lambda_2 \geq \dots$ are the corresponding nonincreasing eigenvalues, and $\xi_{ik} = \int_a^b \{Y_i(s) - \mu(s)\} \phi_k(s) ds$ are uncorrelated random variables with mean 0 and variance λ_k . Moreover, *IEV* assumes that: (3) curves are observed with error, i.e., $\tilde{Y}_i(s) = Y_i(s) + \epsilon_i(s)$, where $\tilde{Y}_i(s)$ are the observed curves and $\epsilon_i(s) \sim N(0, \sigma^2)$ is the measurement error; (4) $\tilde{Y}_i(s)$ are measured on subject specific finite grids $\mathbf{s}_i = \{s_{ij}\}_{j=1}^{J_i}$ that are often irregularly spaced and/or sparse. Note that J_i is the number of observations per curve and it is subject dependent. Under these conditions, Goldsmith et al. (2013) propose to estimate $\mu(s)$ using penalized splines fit to the pooled observations under working independence and construct $\tilde{\Sigma}^{\mathbf{Y}}(s, s')$, a raw estimate of the covariance matrix, using a method of moments approach combined with a smoothing step for its off-diagonal elements. Then, the spectral decomposition of $\tilde{\Sigma}^{\mathbf{Y}}(s, s')$ allows them to obtain the estimated principal component basis functions $\hat{\phi}(s) = \{\hat{\phi}_k(s) : k \in \{1, \dots, \hat{K}\}\}$ and score variances $\{\hat{\lambda}_k(s) : k \in \{1, \dots, \hat{K}\}\}$, where \hat{K} is the minimum number of components needed to explain 99% of the variability in the data. They define the final estimation of the covariance matrix as

$$\hat{\Sigma}^{\mathbf{Y}}(s, s') = \sum_{k=1}^{\hat{K}} \hat{\lambda}_k \hat{\phi}_k(s) \hat{\phi}_k(s') = \hat{\phi}(s) \hat{\Lambda} \hat{\phi}^T(s'), \quad (8)$$

where $\hat{\Lambda}$ is a diagonal matrix with elements $\hat{\lambda}_1(s), \dots, \hat{\lambda}_{\hat{K}}(s)$. Moreover, they estimate σ^2

as the average difference between the middle 60% diagonal elements of the raw covariance matrix and $\hat{\Sigma}^{\mathbf{Y}}(s, s')$.

Following Yao et al. (2005), *IEV* assumes a mixed model framework to predict scores. Given that

$$\tilde{Y}_i(s_{ij}) = \mu(s_{ij}) + \sum_{k=1}^K \xi_{ik} \phi_k(s_{ij}) + \epsilon_i(s_{ij}), \quad (9)$$

and

$$\boldsymbol{\xi}_i \stackrel{iid}{\sim} N[0, \Lambda], \quad \epsilon_i(s_{ij}) \stackrel{iid}{\sim} N[0, \sigma^2], \quad (10)$$

where $\boldsymbol{\xi}_i = \{\xi_{ik} : k \in \{1, \dots, K\}\}$ and $\epsilon_i = \{\epsilon_i(s_{i1}), \dots, \epsilon_i(s_{iJ_i})\}$ are independent, the scores can be estimated using their Best Linear Unbiased Predictions (BLUPs), i.e.,

$$\hat{\boldsymbol{\xi}}_{\hat{\boldsymbol{\theta}}, i} = E \left[\boldsymbol{\xi}_i \mid \tilde{Y}_i(\mathbf{s}_i), \hat{\boldsymbol{\theta}} \right] = \left(\hat{\boldsymbol{\phi}}^T(\mathbf{s}_i) \hat{\boldsymbol{\phi}}(\mathbf{s}_i) + \hat{\sigma}^2 \hat{\Lambda}^{-1} \right)^{-1} \times \hat{\boldsymbol{\phi}}^T(\mathbf{s}_i) \left(\tilde{Y}_i(\mathbf{s}_i) - \hat{\mu}(\mathbf{s}_i) \right), \quad (11)$$

where $\boldsymbol{\theta} = \{\boldsymbol{\phi}(s), \mu(s), \Lambda, \sigma^2, K\}$ is the collection of unobserved FPC decomposition objects, $\hat{\boldsymbol{\theta}}$ is its estimate, and $\tilde{Y}_i(\mathbf{s}_i)$, $\hat{\boldsymbol{\phi}}(\mathbf{s}_i)$ and $\hat{\mu}(\mathbf{s}_i)$ are the vector of observations for curve i , the $J_i \times K$ matrix containing the collection of estimated basis functions evaluated at \mathbf{s}_i and the estimated mean function evaluated at \mathbf{s}_i , respectively.

Given a particular decomposition, the method proposed by Yao et al. (2005) provides not only the scores estimates in (11), but also the estimate of Y_i over the dense grid \mathbf{s}_g as

$$\hat{Y}_{\hat{\boldsymbol{\theta}}, i}(\mathbf{s}_g) = E \left[\tilde{Y}_i(\mathbf{s}_g) \mid \hat{\boldsymbol{\xi}}_{\hat{\boldsymbol{\theta}}, i}, \hat{\boldsymbol{\theta}} \right] = \hat{\mu}(\mathbf{s}_g) + \hat{\boldsymbol{\phi}}(\mathbf{s}_g) \hat{\boldsymbol{\xi}}_{\hat{\boldsymbol{\theta}}, i}, \quad (12)$$

where \mathbf{s}_g is often taken as the union of the \mathbf{s}_i , while the covariance operator of (12) is given

by

$$Var \left[\hat{Y}_{\hat{\theta},i}(\mathbf{s}_g) - Y_i(\mathbf{s}_g) \mid \hat{\theta} \right] \approx \hat{\phi}(\mathbf{s}_g) \left(\frac{1}{\hat{\sigma}^2} \hat{\phi}^T(\mathbf{s}_i) \hat{\phi}(\mathbf{s}_i) + \hat{\Lambda}^{-1} \right)^{-1} \hat{\phi}^T(\mathbf{s}_g). \quad (13)$$

Using (12) and (13), Yao et al. (2005) derived the $100(1 - \alpha)\%$ point-wise confidence intervals for $\hat{Y}_{\hat{\theta},i}(\mathbf{s}_g)$ in the following way:

$$\hat{Y}_{\hat{\theta},i}(\mathbf{s}_g) \pm \Phi^{-1} \left(1 - \frac{\alpha}{2} \right) \sqrt{\text{diag} \left\{ Var \left[\hat{Y}_{\hat{\theta},i}(\mathbf{s}_g) - Y_i(\mathbf{s}_g) \mid \hat{\theta} \right] \right\}}, \quad (14)$$

where $\Phi(\cdot)$ is the standard Gaussian cumulative distribution function.

IEV modifies the previous procedure by implementing a bootstrap step to take into account PCA decomposition-based uncertainty. In the *IEV* method, bootstrap samples are obtained by resampling curves with replacement. Given the b th bootstrap sample $\tilde{\mathbf{Y}}_b$, they derive the bootstrap analogues of (8) and $\hat{\theta}$, denoted as $\hat{\Sigma}_b^{\mathbf{Y}}$ and $\hat{\theta}_b$. Conditioning on $\hat{\theta}_b$, the bootstrap analogues of (11), (12) and (13), i.e., $\hat{\xi}_{\hat{\theta}_b,i}$, $\hat{Y}_{\hat{\theta}_b,i}(\mathbf{s}_g)$ and $Var \left[\hat{Y}_{\hat{\theta}_b,i}(\mathbf{s}_g) - Y_i(\mathbf{s}_g) \mid \hat{\theta}_b \right]$, for each element of the full data set $\tilde{\mathbf{Y}}$ can be obtained. Finally, they combine information across bootstrap samples to estimate curves and construct variability estimates. Using the iterated expectation formula, the estimate of $Y_i(s)$ over the dense grid \mathbf{s}_g is given by

$$\hat{Y}_i(\mathbf{s}_g) = E_{\hat{\theta}} \left\{ E_{\tilde{Y}_i | \hat{\theta}} \left[\tilde{Y}_i(\mathbf{s}_g) \mid \hat{\xi}_{\hat{\theta},i}, \hat{\theta} \right] \right\}, \quad (15)$$

and using the iterated variance formula, the total covariance operator of the estimated curves is given by:

$$Var \left[\hat{Y}_{\hat{\boldsymbol{\theta}},i}(\mathbf{s}_g) - Y_i(\mathbf{s}_g) \right] = E_{\hat{\boldsymbol{\theta}}} \left[Var_{\hat{Y}|\hat{\boldsymbol{\theta}}} \left(\hat{Y}_{\hat{\boldsymbol{\theta}},i}(\mathbf{s}_g) - Y_i(\mathbf{s}_g) \mid \hat{\boldsymbol{\theta}} \right) \right] + Var_{\hat{\boldsymbol{\theta}}} \left[E_{\hat{Y}|\hat{\boldsymbol{\theta}}} \left(\hat{Y}_{\hat{\boldsymbol{\theta}},i}(\mathbf{s}_g) - Y_i(\mathbf{s}_g) \mid \hat{\boldsymbol{\theta}} \right) \right]. \quad (16)$$

For a confidence level $100(1-\alpha)\%$, Goldsmith et al. (2013) obtained (point-wise) confidence intervals for $\hat{Y}_i(\mathbf{s}_g)$ in the following way:

$$\hat{Y}_i(\mathbf{s}_g) \pm \Phi^{-1} \left(1 - \frac{\alpha}{2} \right) \sqrt{\text{diag} \left\{ Var \left[\hat{Y}_i(\mathbf{s}_g) - Y_i(\mathbf{s}_g) \right] \right\}}. \quad (17)$$

Note that (17) is based on $Var \left[\hat{Y}_i(\mathbf{s}_g) - Y_i(\mathbf{s}_g) \right]$, which is approximated by $Var \left[\hat{Y}_{\hat{\boldsymbol{\theta}},i}(\mathbf{s}_g) - Y_i(\mathbf{s}_g) \right]$. The width of this confidence interval is subject dependent and will vary depending on the sparsity of the specific observation. Given an α , those curves observed at fewer points will have a wider confidence interval indicating more uncertainty in the estimation.

B Simulation study: figures for models 2, 3 and 4

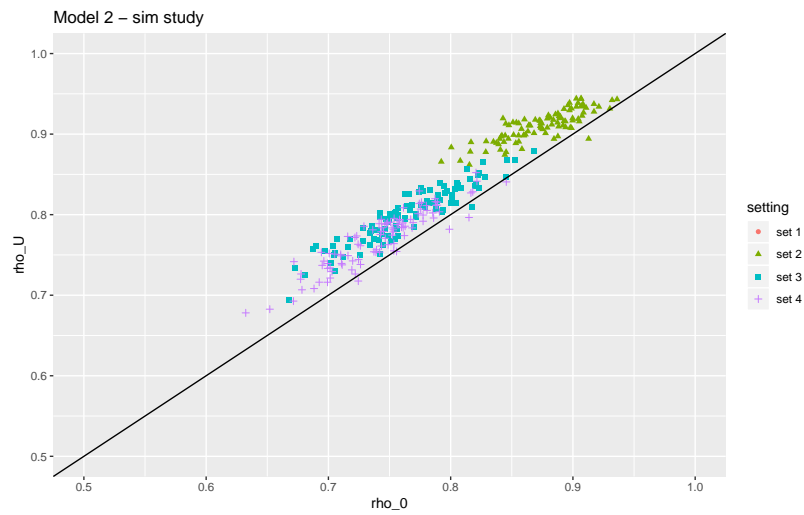


Figure 8: Model 2: scatter plot of (ρ_0, ρ_U) under settings 1-4.

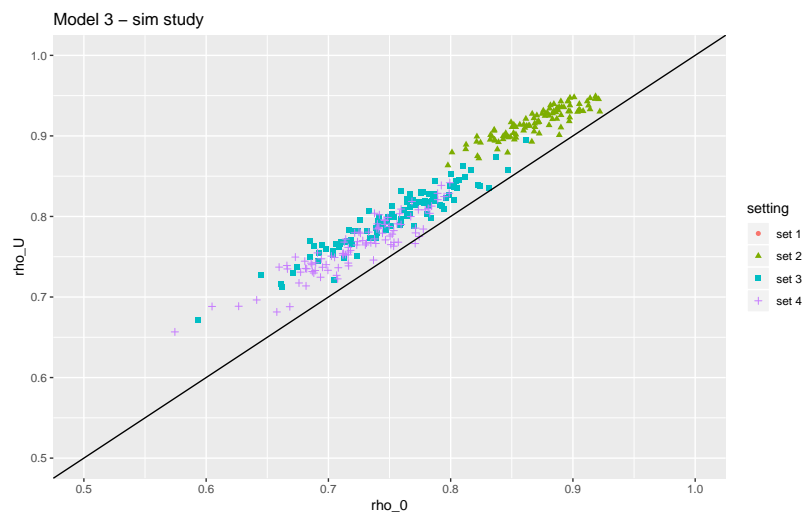


Figure 9: Model 3: scatter plot of (ρ_0, ρ_U) under settings 1-4.

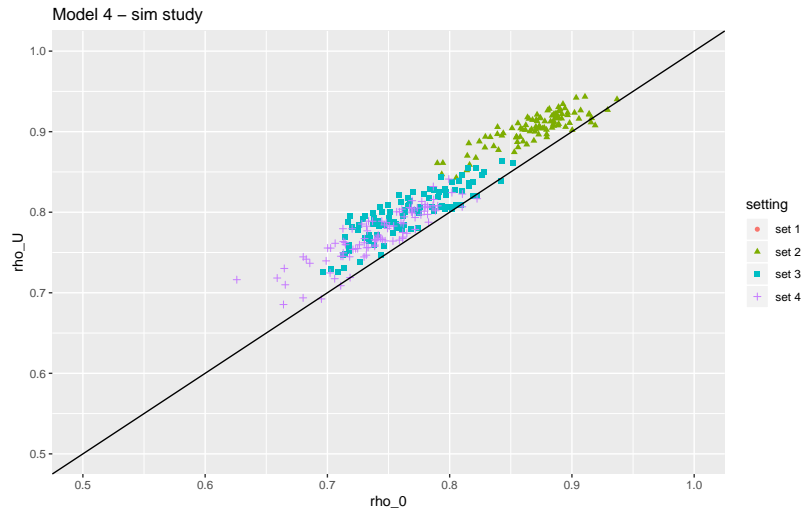


Figure 10: Model 4: scatter plot of (ρ_0, ρ_U) under settings 1-4.

References

- Arribas-Gil, A. and J. Romo (2014). Shape outlier detection and visualization for functional data: the outliergram. *Biostatistics* 15(4), 603–619.
- Azcorra, A., L. F. Chiroque, R. Cuevas, A. F. Anta, H. Laniado, R. E. Lillo, J. Romo, and C. Sguera (2018). Unsupervised scalable statistical method for identifying influential users in online social networks. *Scientific reports* 8(1), 6955.
- Carey, J. R., P. Liedo, H.-G. Müller, J.-L. Wang, and J.-M. Chiou (1998). Relationship of age patterns of fecundity to mortality, longevity, and lifetime reproduction in a large cohort of mediterranean fruit fly females. *The Journals of Gerontology Series A: Biological Sciences and Medical Sciences* 53(4), B245–B251.
- Chakraborty, A. and P. Chaudhuri (2014). On data depth in infinite dimensional spaces. *Annals of the Institute of Statistical Mathematics* 66(2), 303–324.
- Chaudhuri, P. (1996). On a geometric notion of quantiles for multivariate data. *Journal of the American Statistical Association* 91(434), 862–872.
- Cuesta-Albertos, J. A., M. Febrero-Bande, and M. O. de la Fuente (2017). The ddg-classifier in the functional setting. *Test* 26(1), 119–142.
- Cuesta-Albertos, J. A. and A. Nieto-Reyes (2008). The random tukey depth. *Computational Statistics & Data Analysis* 52(11), 4979–4988.
- Cuevas, A., M. Febrero, and R. Fraiman (2007). Robust estimation and classification for functional data via projection-based depth notions. *Computational Statistics* 22(3), 481–496.

- Dai, W. and M. G. Genton (2017). An outlyingness matrix for multivariate functional data classification. *arXiv preprint arXiv:1704.02568*.
- Flores, R., R. Lillo, and J. Romo (2018). Homogeneity test for functional data. *Journal of Applied Statistics* 45(5), 868–883.
- Fraiman, R. and G. Muniz (2001). Trimmed means for functional data. *Test* 10(2), 419–440.
- Gervini, D. (2012). Outlier detection and trimmed estimation for general functional data. *Statistica Sinica*, 1639–1660.
- Gijbels, I. and S. Nagy (2017). On a general definition of depth for functional data. *Statistical Science* 32(4), 630–639.
- Goldsmith, J., S. Greven, and C. M. Crainiceanu (2013). Corrected confidence bands for functional data using principal components. *Biometrics* 69(1), 41–51.
- Hubert, M., P. J. Rousseeuw, and P. Segaeert (2015). Multivariate functional outlier detection. *Statistical Methods & Applications* 24(2), 177–202.
- Jörnsten, R. (2004). Clustering and classification based on the l1 data depth. *Journal of Multivariate Analysis* 90(1), 67–89.
- Koshevoy, G., K. Mosler, et al. (1997). Zonoid trimming for multivariate distributions. *The Annals of Statistics* 25(5), 1998–2017.
- Li, J., J. A. Cuesta-Albertos, and R. Y. Liu (2012). Dd-classifier: Nonparametric classification procedure based on dd-plot. *Journal of the American Statistical Association* 107(498), 737–753.

- Liu, R. Y. et al. (1990). On a notion of data depth based on random simplices. *The Annals of Statistics* 18(1), 405–414.
- Liu, R. Y., J. M. Parelius, K. Singh, et al. (1999). Multivariate analysis by data depth: descriptive statistics, graphics and inference,(with discussion and a rejoinder by liu and singh). *The annals of statistics* 27(3), 783–858.
- Liu, R. Y. and K. Singh (1993). A quality index based on data depth and multivariate rank tests. *Journal of the American Statistical Association* 88(421), 252–260.
- López-Pintado, S. and R. Jornsten (2007). Functional analysis via extensions of the band depth. *Lecture Notes-Monograph Series*, 103–120.
- López-Pintado, S. and J. Romo (2007). Depth-based inference for functional data. *Computational Statistics & Data Analysis* 51(10), 4957–4968.
- López-Pintado, S. and J. Romo (2009). On the concept of depth for functional data. *Journal of the American Statistical Association* 104(486), 718–734.
- López-Pintado, S. and J. Romo (2011). A half-region depth for functional data. *Computational Statistics & Data Analysis* 55(4), 1679–1695.
- López-Pintado, S. and Y. Wei (2011). Depth for sparse functional data. In *Recent advances in functional data analysis and related topics*, pp. 209–212. Springer.
- López-Pintado, S. and J. Wrobel (2017). Robust non-parametric tests for imaging data based on data depth. *Stat* 6(1), 405–419.
- Mahalanobis, P. C. (1936). On the generalized distance in statistics. National Institute of Science of India.

- Mosler, K. and Y. Polyakova (2012). General notions of depth for functional data. *arXiv preprint arXiv:1208.1981*.
- Narisetty, N. N. and V. N. Nair (2016). Extremal depth for functional data and applications. *Journal of the American Statistical Association* 111(516), 1705–1714.
- Nieto-Reyes, A. and H. Battey (2016). A topologically valid definition of depth for functional data. *Statistical Science*, 61–79.
- Oja, H. (1983). Descriptive statistics for multivariate distributions. *Statistics & Probability Letters* 1(6), 327–332.
- Rousseeuw, P. J. and M. Hubert (1999). Regression depth. *Journal of the American Statistical Association* 94(446), 388–402.
- Sguera, C., P. Galeano, and R. Lillo (2014). Spatial depth-based classification for functional data. *Test* 23(4), 725–750.
- Sguera, C., P. Galeano, and R. E. Lillo (2016). Functional outlier detection by a local depth with application to no x levels. *Stochastic environmental research and risk assessment* 30(4), 1115–1130.
- Sun, Y. and M. G. Genton (2011). Functional boxplots. *Journal of Computational and Graphical Statistics* 20(2), 316–334.
- Sun, Y. and M. G. Genton (2012). Functional median polish. *Journal of agricultural, biological, and environmental statistics* 17(3), 354–376.
- Tukey, J. W. (1975). Mathematics and the picturing of data. In *Proceedings of the International Congress of Mathematicians, Vancouver, 1975*, Volume 2, pp. 523–531.

- Vardi, Y. and C.-H. Zhang (2000). The multivariate l1-median and associated data depth. *Proceedings of the National Academy of Sciences* 97(4), 1423–1426.
- Yao, F., H.-G. Müller, and J.-L. Wang (2005). Functional data analysis for sparse longitudinal data. *Journal of the American Statistical Association* 100(470), 577–590.
- Zhang, X. and J.-L. Wang (2016). From sparse to dense functional data and beyond. *The Annals of Statistics* 44(5), 2281–2321.
- Zuo, Y. (2003). Projection-based depth functions and associated medians. *The Annals of Statistics* 31(5), 1460–1490.
- Zuo, Y. and R. Serfling (2000). General notions of statistical depth function. *Annals of statistics*, 461–482.